



CALCULATION PREDICTION OF FATIGUE LIFE OF FREIGHT CAR SIDE FRAME UNDER ALTERNATING CYCLIC LOADS

V.I. MAKHNENKO and I.Yu. ROMANOVA

E.O. Paton Electric Welding Institute, NASU, Kiev, Ukraine

An example of calculation prediction of fatigue crack growth in a side frame of freight cars at a preset range of random cyclic loads is considered. Relationship between exceeding design conditions of operation of the car and probable cause of its fracture was studied.

Keywords: *fatigue crack, random cyclic loading, side frame, freight car, casting defect, calculation prediction of fatigue life*

In connection with increased scope of railway freight traffic, more attention is given to the «viability» of various parts and components of load-carrying elements of freight cars. Experience of operation of structures developed in Ukraine and Russia is indicative of insufficient cyclic strength of individual components, which results in failure of cars which have not yet completed their design life period [1].

Let us consider a real case of failure of a cast side frame of a freight car (Kabakly Station, West-Siberian Railway, RF, 2009), designed in keeping with [2] and manufactured at OJSC «Azovmash» (Mariupol, Ukraine). Fracture occurred as a result of fatigue crack growth from a technological defect.

Initial information on the fractured side frame is as follows: material is steel of 20GFL type; car run to fracture $L = 108,482$ km; design average technical speed of car movement $\bar{v} = 22.4$ m/s; average daily run of a loaded car $L_d = 210$ km/d; effective frequency of car vertical oscillations $f_e = 2.23$ Hz; coefficient of run in the loaded condition $K = 0.6$; average daily number of cycles under load $N_d = (L_d/\bar{v})10^3 f_e = 20,906$ cycle/d; number of cycles under load during run L to fracture $N = (LK\bar{v})10^3 f_e = 6.48 \cdot 10^6$ cycles; current evaluating repairs were performed at $N_{rep} = N - N_d \cdot 9.5 \cdot 30K = 2.91 \cdot 10^6$ cycles.

Figure 1 shows fracture of a failed frame, and arrows indicate sites of fatigue fracture initiation [3]. According to this work, the site of initiation of a primary fatigue crack (#1 in Figure 1) was a casting defect — surface blowhole, having the length of 2.6 mm, depth of 1.8 mm in the fracture section and located at 31 mm distance from the surface of the outer vertical wall of the side frame. The defect was not detected by NDT means. Site of initiation of secondary fatigue cracks were casting blowholes located at 66, 104 and 125 mm distance from the surface of outer vertical wall and having the dimensions of 2.0×1.5 mm (#2), 4.3×2.3 mm (#4) and 4.0×1.3 mm (#5) in the fracture section. In addition, there is a

surface defect of 3.0×2.0 mm size (#3 in Figure 1), not specified by the drawing of the technological stiffener, which in [3] is regarded as the site of secondary fatigue cracks formation.

Thus, five sites of fatigue fracture are located in the fracture section on the surface with the maximum operating longitudinal stresses, which sufficiently conservatively can be described by semi-elliptical cracks of $2ca$ size, where $2c$ is the crack length along the free surface, and a is the crack depth.

Table 1 gives the initial dimensions of such defects and shows the distance from defect centers to the free vertical surface, as well as the distance between the edges of adjacent defects (L_{n-1} on the left, L_{n+1} on the right), in the initial condition and characteristic parameter b of interaction with adjacent defects:

$$b = c + \min \begin{cases} L_{n-1, n} \\ L_{n+1, n} \end{cases}$$

or the free edge (vertical free surface). In [13] it is noted that the described casting contamination defects were evaluated in terms of their admissibility (inadmissibility) based on the principles (approaches) of fracture mechanics of cracked solids, described for the case considered in [4]. From this assessment it follows that the described casting defects are inadmissible, as under the design operation conditions during three years they grow by the fatigue mechanism to dimensions, at which their progressive growth begins, leading to fracture after approximately 2.9 months of service. Unfortunately, absence of such substantiation after the assessment performed in [3], in view of the design conditions of frame loading, gives rise to some doubts as to determination of the main cause for its fracture, so that PWI conducted a study, the essence of which is as follows.

For the above described defects (Table 1) their loading by the spectrum of random cyclic loads described in [2] was considered for average speed of train movement $\bar{v} = 22.4$ m/s at static stresses in the defect zone in the range from $\sigma_{st} = 105.2$ MPa (#1) to $\sigma_{st} = 93.2$ MPa (#2–5), which is in good agreement with the data of [4], where values of the above characteristics are equal to 80–90 MPa.

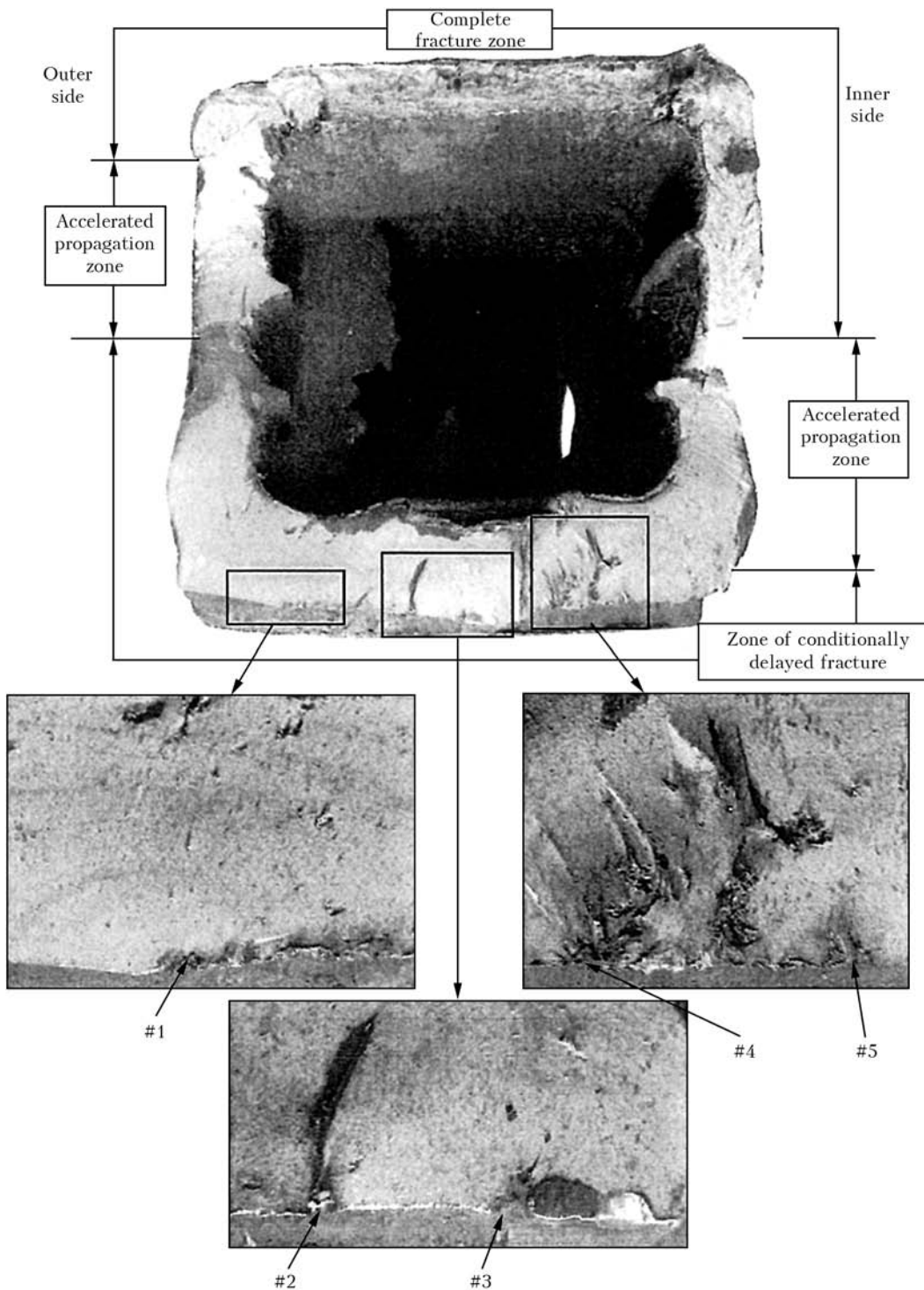


Figure 1. Fracture of side frame of freight car (#1-5 – sites of fatigue crack initiation)

Calculation of dynamic index K_{dyn} , depending on variation of movement speed v is performed according to [2] at static deflection of spring suspension $f_{st} = 0.049$ m (Table 2).

Amplitude of dynamic (cyclic) stresses was determined from the expression

$$\sigma_a = \sigma_{st} K_{dyn} \quad (1)$$

depending on the train movement speed v_i , the value of which is determined within the ranges indicated in Table 2 at probability P_i in the basic loading cycle

N_b , i.e. N_i for the i -th element of loading spectrum in the following form:

$$N_i = N_b P_i \quad (2)$$

It is assumed that in each element of the spectrum $\sigma_{max} = \sigma_{st}$, i.e. coefficient of asymmetry R_i for the i -th element of the loading spectrum is equal to

$$R_i = (1-2)K_{dyni} \quad (3)$$

The rate of growth of the initial crack dimensions $l = a, c$ at the specified load is determined by the



Table 1. Initial dimensions of defect and distance from defect centers to free vertical surface according to [3]

Defect #	Defect parameter, mm					
	2c	a	L ₁	L _{n-1}	L _{n+1}	b
1	2.6	1.8	31	29.7	22.7	24.0
2	2.0	1.5	66	22.7	22.5	23.5
3	3.0	2.0	86	22.5	14.4	15.9
4	4.3	2.3	104	14.4	16.6	15.5
5	4.0	1.3	125	16.6	23.0	18.6

diagram of cyclic crack resistance of steel, a section of which for the considered material of the side frame is given in Figure 2, i.e. it is determined by the range of values of stress intensity factors ΔK_I and loading asymmetry R .

For a broad class of medium-carbon steels such a diagram only slightly depends on the material composition and its microstructure, and various dependencies are used for conservative estimates. According to recommendations of [5], it is rational to apply the following dependence:

$$\frac{dl}{dN} = \frac{C_0 \Delta K_I^m}{(1-R) - \frac{\Delta K_I}{K_c}} \text{ at } \Delta K_I > \frac{\Delta K_{th}(R)}{\gamma_m};$$

$$\frac{dl}{dN} = 0 \text{ at } \Delta K_I < \frac{\Delta K_{th}(R)}{\gamma_m},$$

(4)

where $C_0 = 5 \cdot 10^{-13} \text{ mm}/(\text{MPa} \cdot \text{mm}^{1/2})$; $m = 3$; ΔK_{th} is the threshold value of the range of stress intensity factor dependent on R :

$$\Delta K_{th} = (190-144)R, \tag{5}$$

but not less than 62 MPa·mm^{1/2}; K_c is the material fracture toughness (taken at the temperature of -30 °C) equal to 2065 MPa; γ_m is the safety factor according to [5] equal to 1.25 for primary crack #1 and 1.20 for secondary cracks #2-5.

Table 2. Dynamic indices K_{dyn} for design condition of freight car side frame loading

i	v _i , m/s	K _{dyni}	P _i
1	6.25	0.063	0.03
2	13.75	0.138	0.07
3	16.25	0.159	0.09
4	18.75	0.177	0.12
5	21.25	0.196	0.16
6	23.75	0.214	0.19
7	26.25	0.232	0.16
8	28.75	0.250	0.10
9	31.25	0.269	0.06
10	33.75	0.287	0.02

Dependence (4), compared to the data in Figure 2, gives somewhat higher values of the growth rate, which is quite acceptable for conservative estimates.

Parameter ΔK_I is determined for a semi-elliptical crack, according to [5], in the following form:

$$\Delta K_I = 2\sigma_a \sqrt{\frac{\pi a}{Q}} F, \tag{6}$$

where Q and F are calculated by the following dependencies:

$$F = \left[M_1 + M_2 \left(\frac{a}{\delta} \right)^2 + M_3 \left(\frac{a}{\delta} \right)^4 \right] g f_{wf} b,$$

where δ is the wall thickness in the defect zone (taken to be $\delta = 25 \text{ mm}$).

At $a < c$

$$Q = 1 + 1.464 \left(\frac{a}{c} \right)^{1.65}; \quad M_1 = 1.13 - 0.09 \left(\frac{a}{c} \right);$$

$$M_2 = -0.54 + \frac{0.89}{0.2 + \frac{a}{c}};$$

Table 3. Calculation of ΔK and safety factor γ_m for primary crack #1 (according Table 1)

v _i , m/s	K _{dyni}	ΔK_{th} , MPa·mm ^{1/2}	$\Delta\sigma$, MPa	$\Delta K_I(a)$	$\gamma_m(a)$	$\Delta K_I(c)$	$\gamma_m(c)$
6.25	0.063	64.1	13.25	17.2	3.73	22.3	2.88
13.75	0.138	85.7	29.03	37.7	2.27	48.8	1.75
16.25	0.159	91.8	33.45	43.4	2.11	56.3	1.63
18.75	0.177	97.0	37.24	48.3	2.00	62.6	1.55
21.25	0.196	102.4	41.24	53.5	1.91	69.3	1.48
23.75	0.214	107.6	45.02	58.4	1.84	75.7	1.42
26.25	0.232	112.8	48.81	63.3	1.78	82.1	1.37
28.75	0.250	118.0	52.60	68.3	1.73	88.5	1.33
31.25	0.269	123.5	56.60	73.4	1.68	95.2	1.29
33.75	0.287	128.6	60.40	78.4	1.64	101.5	1.27



$$M_3 = 0.5 - \frac{1}{0.65 + \frac{a}{c}} + 14 \left(1 - \frac{a}{c}\right)^{24}$$

For parameter a , $g = 1$, $f_b = 1$.
For parameter c

$$g = 1 + \left[0.1 + 0.35 \left(\frac{a}{\delta}\right)^2\right], \quad f_b = \sqrt{a/c}.$$

At $a > c$

$$Q = 1 + 1.464 \left(\frac{c}{a}\right)^{1.65}; \quad M_1 = \left(1 + 0.04 \frac{c}{a}\right) \sqrt{\frac{c}{a}};$$

$$M_2 = 0.2 \left(\frac{c}{a}\right)^4; \quad M_3 = -0.11 \left(\frac{c}{a}\right)^4.$$

For parameter a , $g = 1$, $f_b = \sqrt{c/a}$.

For parameter c , $g = 1 + \left[0.1 + 0.35 \left(\frac{a}{\delta}\right)^2 \left(\frac{c}{a}\right)\right], \quad f_b = 1.$

The rest as for $a/c < 1$.

Dependencies (1)–(6) were used to trace the development of defects (cracks) considered in Table 1 at the design spectrum of train movement speed at $N_b = 6.47 \cdot 10^6$ cycles, i.e. on the base of the real run

dl/dN , m/cycle

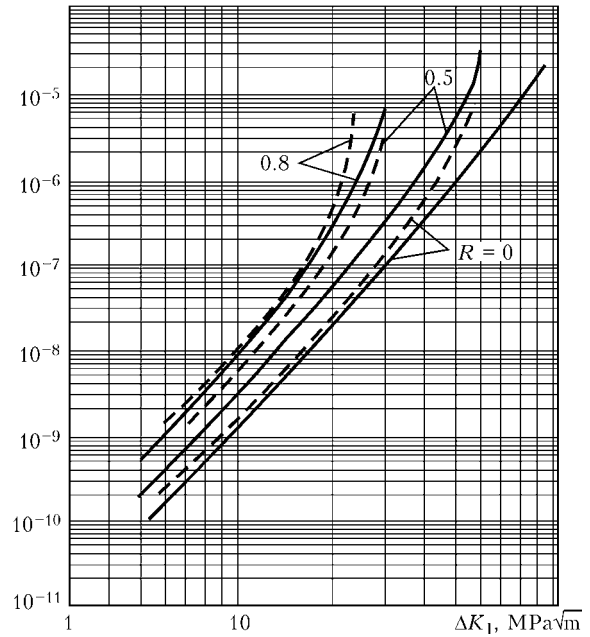
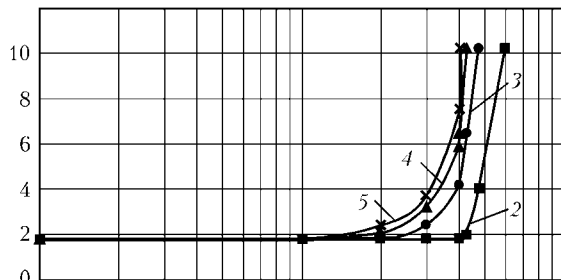


Figure 2. Fatigue fracture diagram of steel at different values of the coefficient of loading asymmetry R [4]

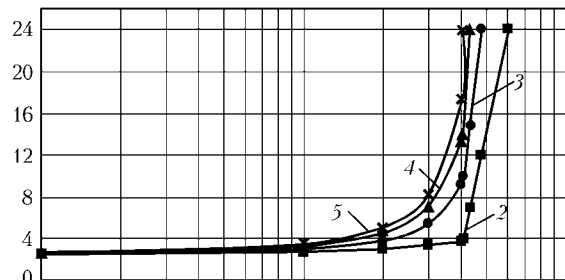
to failure. Dependence determines relative frequency of spectrum elements (2). Randomness of spectrum elements was realized using random-number generator $0 \leq D \leq 1$. A more conservative approach of tracing

a , mm



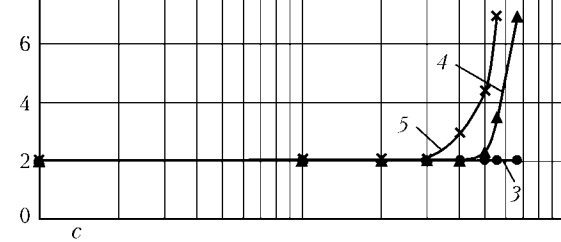
a

$2c$, mm



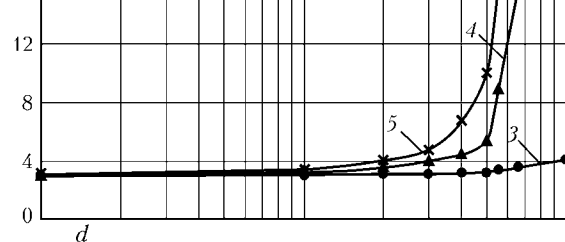
b

c



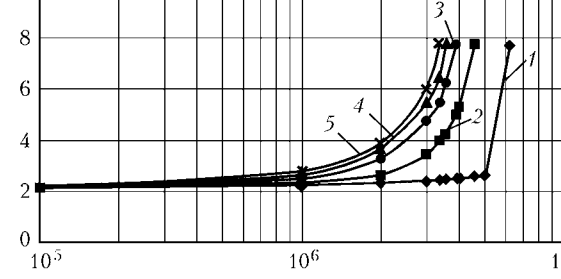
c

d



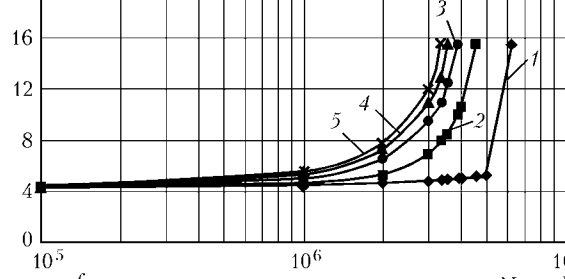
d

e



e

f



f

N , cycle

Figure 3. Kinetics of growth of defects #1 (a , b), #3 (c , d) and #4 (e , f) at car movement at a higher speed depending on safety factor γ_m : a , c , e – increase of crack depth a ; b , d , f – $2c$ growth; 1 – $\gamma_m = 1.20$; 2 – 1.25; 3 – 1.30; 4 – 1.35; 5 – 1.40



through the spectrum was used, starting from high load amplitudes and down to small amplitudes, i.e. starting from $i = 10$ and ending by $i = 1$.

Results of calculation of the kinetics of change of dimensions a and c of the initial defect #1 (cracks) in the design loading spectrum on the base of real fatigue life of the considered side beam showed that during the entire operating period of the car ($N_b = 6.47 \cdot 10^6$ cycles) the initial dimensions of the defect did not change, which is due to inequality $\Delta K_1 < \Delta K_{th} / \gamma_m$ (as shown in Table 3) for each element of the loading spectrum.

A similar situation is in place also for defects #2–5, from which secondary cracks are developing, i.e. under design operating conditions of the train the considered defects are admissible, non the less fracture did take place. Let us prove that the cause for the considered fracture can be inclusion into the loading spectrum of a higher speed of train movement. With this purpose a spectrum of speed according to [2] was considered, which corresponds to the design average technical speed of 24.7 m/s. Figure 3 gives the calculated data on the kinetics of variation of dimensions of defects #1, 3 and 4 at increased (compared to design) movement speed, from which it is seen that appearance of $v = 36.25$ m/s, $P = 0.05$ and $v = 38.75$ m/s, $P = 0.02$ in the speed spectrum noticeably changes the kinetics of the change of dimensions a and c of initial defects (cracks). Calculations showed that defects #2 and 5 do not show any growth at these input parameters. Practically, at $N = 5 \cdot 10^6$ cycles the above defects coalesce, forming a continuous crack about 10 mm deep along the base surface, at which the remaining life of the side beam is quite limited. It is characteristic that at $N = 3 \cdot 10^6$ loading cycles (approximately cor-

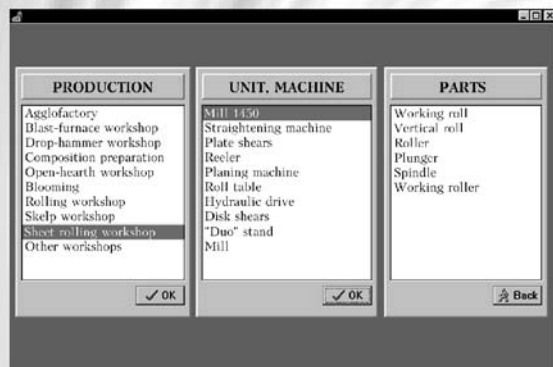
responds to the moment of setout repair 9.5 months before failure) the defects have grown noticeably and they can be detected by the non-destructive methods. Naturally, the considered variant of operation at increased speed is quite hypothetical. It shows that a quite probable cause for fracture could be the accumulated damage related to car operation in modes not envisaged by design.

Thus, calculations show that fatigue fracture of the side frame of a train car occurred because of casting defects-blowholes found in the fracture. These defects as to their geometrical dimensions are admissible at design conditions of car service. However, exceeding the design conditions of the car operation, in particular, its movement speed can be the cause for the considered defect transition into the category of inadmissible defects.

Given calculation algorithms allow prediction of the influence of variable cyclic loads applied randomly, on the growth of fatigue cracks in structural elements of railway cars and predicting their fatigue life.

1. Makhnenko, V.I., Saprykina, G.Yu. (2009) Safety service life of welded joints of bays. In: *Proc. of 4th Int. Conf. on Mathematical Modeling and Information Technologies in Welding and Related Processes* (27–30 May 2008, Katsiveli, Crimea, Ukraine). Kiev: PWI, 103–108.
2. *Codes of structural design of railway cars (non-self-propelled) of Ministry of Communications for track of 1520 mm.* Introd. 07.02.96.
3. (2009) *Technical conclusion on expert verification results in determination of causes of side frame fracture N 36213-143-06 at 2903 km PK7 in Barabinsk-Tatarskaya section behind point #6 of Kabakly station of Novosibirsk Division of West-Siberian Railway of VNIIZhT Company.* Approved 27.02.2009. Moscow.
4. Severinova, T.P. (2002) Design-theoretical substantiation of viability of side frames and bolsters with admissible defects. *Vestnik VNIIZhT*, 5, 40–45.
5. (1996) Recommendation for fatigue design of welded joints and components. *IIV Doc. XIII-1539-96/XV-845-96.*

COMPUTER SYSTEM TO DESIGN TECHNOLOGIES FOR REPAIR AND HARDENING OF METALLURGICAL EQUIPMENT PARTS



Selection of a part to be surfaced

Purpose. The system is intended to design technologies for repair and hardening of metallurgical equipment parts by the electric arc surfacing methods. The computer system is based on the experience accumulated by 16 metallurgical plants in the field of surfacing. It allows design of a surfacing technology for 350 different parts (selection of surfacing consumables, methods, conditions, equipment, etc.) at a level of a highly skilled specialist. The system operation result has the form of a process sheet.

Application. The system can be used at metallurgical enterprises. It is intended for welding technologists working at a plant engineering department.

Contacts: Prof. Makhnenko V.I.
E-mail: d34@paton.kiev.ua